Proceedings of the 32nd European Safety and Reliability Conference (ESREL 2022)
Edited by Maria Chiara Leva, Edoardo Patelli, Luca Podofillini, and Simon Wilson
©2022 ESREL2022 Organizers. *Published by* Research Publishing, Singapore.
doi: 10.3850/978-981-18-5183-4_R22-08-170-cd

Atmospheric Corrosion Prognostics Using a Particle Filter

Luc S. Keizers
Chair of Dynamics Based Maintenance, University of Twente, the Netherlands
Faculty of Military Sciences, Netherlands Defense Academy, the Netherlands
E-mail: *l.s.keizers@utwente.nl*

Richard Loendersloot
Chair of Dynamics Based Maintenance, University of Twente, the Netherlands
E-mail: *r.loendersloot@utwente.nl*

Tiedo Tinga
Chair of Dynamics Based Maintenance, University of Twente, the Netherlands
Faculty of Military Sciences, Netherlands Defense Academy, the Netherlands
E-mail: *t.tinga@utwente.nl*

A prognostic algorithm can guarantee high reliability and availability of machinery of structures at acceptable costs. This paper proposes to use a particle filter for atmospheric corrosion prognostics, which bridges the gap between corrosion *modeling* and corrosion *monitoring*. The applied particle filter only takes temperature and monitored mass loss as input and is based on Arrhenius equation. The output of the particle filter is a probability distribution of the remaining useful life that considers uncertainties on the process, the model and future weather conditions. The effectiveness of the approach is demonstrated by a case study composed from monthly exposure tests performed by the National Institute of Materials Science in Japan. It is shown that the particle filter estimates suitable model parameters of the corrosion model to give good remaining useful life estimations, while only requiring a relatively simple corrosion model. In new practical applications challenges remain in parameter selection and initialization of the algorithm. Furthermore, the method should be validated on an actual long-term corrosion process.

Keywords: Predictive Maintenance, Corrosion, Prognostics, Varying Conditions, Particle Filter

1. Introduction

Corrosion is a process in which metals dissolve at wet surfaces due to electrochemical reactions (Tinga, 2013). Reduced metal thickness leads to deteriorated mechanical properties of machines or structures which can cause unexpected failures with catastrophic and expensive consequences. Failures can be avoided with preventive maintenance actions. However, if these actions are performed too frequently, unnecessary maintenance costs are made and availability of assets decreases. But, if these actions are performed too late, reliability decreases and failures can occur.

The aim of predictive maintenance is to predict failures such that maintenance is only performed when it is essential, increasing the reliability and availability of assets at reduced costs. This can be achieved with prognostic algorithms that calculate when an asset will be in a critical state. Although predictive maintenance and prognostic algorithms gained a lot of research attention, applications to corrosion-affected assets are rather scarce. Related research topics in corrosion science are corrosion *modeling* and *monitoring*. However, the focus of corrosion science is on fundamental understanding of the process and does generally not concern applications for predictive maintenance (Melchers, 2019).

The main challenge in corrosion *modeling* is that corrosion is a very complex physical process. The specific types of electrochemical reactions, and thus corrosion rates, depend on a large number of environmental parameters, and on interactions between those parameters and materials. This makes it practically impossible to predict corrosion rates using physical principles (Tinga,

2013). Therefore, corrosion is often modeled using empirical and statistical models. A variety of corrosion models can be found in literature, from which the power law model is the most commonly used one (Cai et al., 2020).

Such an empirical model is only applicable for the environment in which it was developed and development requires experiments that last multiple years. This makes it an infeasible method for assets in varying conditions, i.e. moving assets. Furthermore, accuracy of these models may decrease over time (e.g. due to climate change). Therefore, attempts have been made to model corrosion rates as a function of environmental parameters using statistical methods or machine learning models (Cai et al., 2020). The capability of machine learning models to reveal hidden patterns in data is promising for a complex phenomenon like corrosion. However, globally applicable corrosion models require large, independent and homogeneous training data sets which are generally not available for corrosion (Melchers, 2019), limiting their applicability.

Corrosion *monitoring* can provide diagnostic information about the state of an asset. For example, ultrasonic sensors can be used to assess the wall thickness of a corroding asset or galvanic current measurements can provide information on the number of electrochemical reactions (Pei et al., 2021). However, these sensors are practically not used in combination with a prognostic step due to the complexity of the corrosion predictions (Melchers, 2019).

Thus, on the one hand there are corrosion models available which are not widely applicable due to their empirical nature and the limited amount of model training data. On the other hand, corrosion monitoring devices are available, which provide real-time corrosion data but do not include predictions. This paper proposes to combine these two worlds in a prognostic framework using a Bayesian filter, the particle filter (PF). This approach is suitable because a PF 1) is a tool to track noisy and uncertain processes and 2) learns in real-time, such that it does not require large, historical training data sets. The PF is applied to a data set that is constructed using data from monthly exposure tests performed by the National Institute for Materials Science in Japan (NIMS, 2011). Because of seasonal effects, the influence of a varying environment is included in this data set.

The remainder of this paper is organized as follows. Section 2 introduces the case. Section 3 introduces the principle and the initialization of the algorithm. Section 4 presents the results. Section 5 discusses the method and section 6 concludes the paper.

2. Case Study

NIMS (2011) performed monthly exposure tests in Tsukuba, Japan. Sets of three carbon steel test coupons were exposed to the atmosphere for one month consecutively, during a period of two years starting from April 2007. Corrosion products are removed after one month and the coupons mass is measured, such that the mass loss due to corrosion could be estimated. Also the monthly average temperature, relative humidity, chloride deposition rate and sulfur dioxide deposition rate as well as the total amount of precipitation were monitored and registered.

In this paper a continuous corrosion process will be simulated. To get a data set representative for a continuous process, the mass loss measurement of one of the three test coupons is selected for each month. Then, the accumulated mass loss up till that month is calculated. To create more data points, the data set is duplicated such that two times 24 months are represented. This yields the data set as shown in Fig. 1.

Long-term corrosion effects are not modeled in this work. In a real continuous corrosion process a protective (rust) layer can form on the metal surface, decreasing the corrosion rate. Because coupons are replaced after each month, the effect of such a layer is not included. This limitation will be discussed in section 5. However, varying conditions are included as higher corrosion rates are observed during the warmer months. This makes the data set suitable to demonstrate the effectiveness of a PF for corrosion predictions in varying conditions.

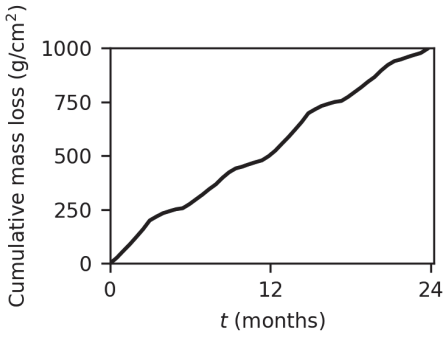

Fig. 1.: The constructed data set using monthly exposure data of (NIMS, 2011).

3. Methodology

This section explains the principle of a PF. Then, it is explained how it is initialized for corrosion prediction and how prognostics are performed.

3.1. *Particle filter algorithm*

The PF constructs a posterior probability distribution of a state from a noisy process, given a noisy measurement. This is accomplished by applying Bayes' rule, which can be written as follows (Arulampalam et al., 2002):

$$p\left(x_k|z_{1:k}\right) = \frac{p\left(z_k|x_k\right)p\left(x_k|z_{1:k-1}\right)}{\int p\left(z_k|x_k\right)p\left(x_k|z_{1:k-1}\right)dx} \quad (1)$$

in which $p\left(x_k|z_{1:k}\right)$ is the posterior, $p\left(z_k|x_k\right)$ is the likelihood, $p(x_k|z_{1:k-1})$ is the prior and $\int p\left(z_k|x_k\right)p\left(x_k|z_{1:k-1}\right)$ is a normalization factor. In the context of corrosion, the likelihood is obtained from a measurement of the actual mass loss and the prior is calculated using a corrosion model.

Eq. (1) cannot be solved analytically for non-linear and non-Gaussian problems. Therefore, the PF approximates the posterior distribution as a discrete set of weighted particles using Monte-Carlo simulations (Chen, 2003). A schematic overview of the PF utilized in this work is visualized in Fig. 2. In the state transition step (a-b) a state transition model $f\left(x_{k-1}, w_k\right)$ predicts the prior distribution of the state in the current time step from the previous state x_{k-1} and a process noise w_k. Then the update stage takes

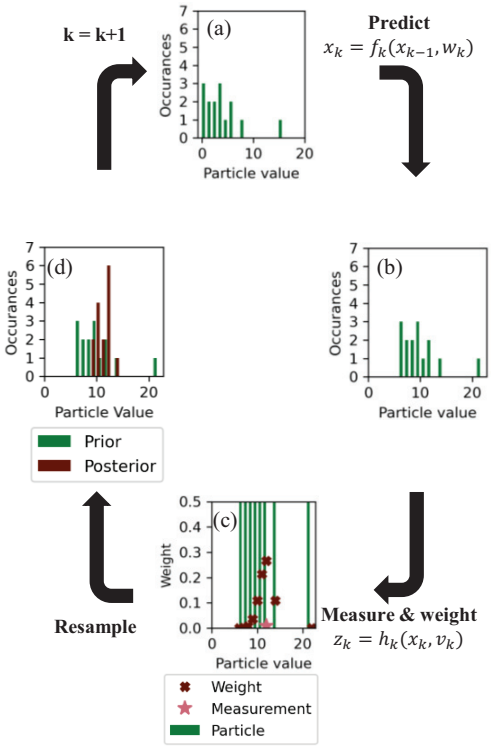

Fig. 2.: Schematic overview of the PF with a) the probability distribution of the state at $t = k-1$, b) the prior distribution of the state at $t = k$, c) the weights of the prior particles at k, given the measurement and d) the posterior distribution of the state at $t = k$.

place (b-d). In this stage, first a measurement model ($h_k\left(x_k, v_k\right)$) matches the predicted state (x_k) with the received measurement, considering measurement noise v_k (i.e. if the state is measured indirectly, a conversion is required to compare the predicted with the measured state). Then the particles in the prior are weighted proportional to he received measurement (b-c). The weights are used for resampling (c-d), where particles with low weights are removed and replaced by particles with high weights, such that only prior particles that correspond to the measurement survive. This yields the posterior distribution, which is selected as initial distribution for the next time step (d-

a). More detailed explanations, the derivation and variations of the PF can be found in literature, e.g. Arulampalam et al. (2002) or Elfring et al. (2021).

Fig. 2 explains the principle of the PF using a 1D particle. However, the state can consist of multiple dimensions. For prognostics it is helpful to also update model parameters, such that predictions can be done using updated model parameters. This can be achieved by creating a vector $\boldsymbol{x}$ with a state (vector) $\boldsymbol{s}$ and a parameter (vector) $\boldsymbol{\theta}$, i.e.:

$$\boldsymbol{x} = \left\{\boldsymbol{s}, \boldsymbol{\theta}\right\}^{\boldsymbol{T}} \tag{2}$$

3.2. *Particle filter initialization*

This section first introduces the state transition model and the measurement model. Then the number of particles, the prior and the process noises are given. Lastly it is explained how prognostics are performed.

State transition model The state transition model is based on a multi-factor combination model. This type of corrosion model predicts mass loss using accelerating factors for environmental parameters (Cai et al., 2020). In this work an accelerating factor for temperature was selected for the state transition model, because the data set (NIMS, 2011) suggests a high correlation between temperature and mass loss. A common way to include temperature in a corrosion model is using the Arrhenius equation (Cai et al., 2021). This equation states that more electrochemical reactions occur at higher temperatures (Arrhenius, 1889). The state transition function including the Arrhenius equation is described as follows:

$$C_k = C_{k-1} + k_{nom} \cdot \exp\left(\beta_{k-1}\left(\frac{1}{T_k} - \frac{1}{T_{nom}}\right)\right)\Phi_{k-1} + \varepsilon_{C,k} \tag{3a}$$

$$\beta_k = \beta_{k-1} + \varepsilon_{\beta,k} \tag{3b}$$

$$\Phi_k = \Phi_{k-1} + \varepsilon_{\Phi,k} \tag{3c}$$

with C the mass loss, k_{nom} and T_{nom} the nominal mass loss and temperature respectively, T_k the input temperature, β and Φ model parameters and ε the process noises. Eq. 3a basically multiplies k_{nom} by a value > 1 when $T_k > T_{nom}$ and by a value < 1 when $T_k < T_{nom}$. The input temperatures are measured each month by (NIMS, 2011) and are given in Table 1.

Because k_{nom} and T_{nom} are not known and need to be approximated, the exponential function is multiplied by correction factor Φ. k_{nom} and T_{nom} are approximated by taking the average monthly mass loss and temperature from a worldwide corrosion database (ICP, 1987) for non-marine environments (the subset created by Chico et al. (2017) has been used).

Measurement model Also the measurement model needs to be defined. Because direct mass loss measurements are available NIMS (2011), the measurement model is described by:

$$z_k = x_k \tag{4}$$

and assuming a Gaussian measurement error the likelihood is defined as follows:

$$p\left(y_k|x_k\right) \sim \mathcal{N}\left(z_k, \sigma_v^2\right) \tag{5}$$

such that the weights can be computed by:

$$w_k^i = \frac{1}{\sigma_v\sqrt{2\pi}}\exp\left(-\frac{1}{2}\left(\frac{z_k - C_k^i}{\sigma_v}\right)^2\right) \tag{6}$$

with $\sigma_v = 0.01$ the measurement noise.

Filter settings The number of particles, initial priors (distributions before the first state transition) and process noises need to be defined. This is preferably done from (physical) knowledge of the process, which in this case is difficult due to the complex physics involved. In this work they are selected based on a trade-off between robustness and accuracy of the PF. In section 5 filter initialization for new practical applications will be discussed. The initial priors and process noises are given in Table 2.

The number of particles is not only a trade-off between robustness and accuracy, but also affects the computational effort of the algorithm. A total number of 10^5 particles was selected. From this number, consistent results were obtained with acceptable errors and decent computational times.

Table 1.: Monthly average temperature data for Tsukuba, Japan. During the filtering stage the input temperature was measured (year 1 and year 2) (Retrieved from NIMS (2011)) and for the prognostic stage input temperature values were drawn from a Gaussian with parameters μ_T and σ_T (Estimated using Weather Atlas (2022))

Temperatures used in PF (in K)	Apr	May	June	July	Aug	Sep	Oct	Nov	Dec	Jan	Feb	Mar
Measured (filtering stage)												
Year 1	285.2	290.7	294.5	295.3	300.1	296.2	289.7	284.2	280.8	276.6	276.7	281.4
Year 2	285.7	289.7	292.6	297.8	298.1	295.3	190.1	283.8	280.3	277.4	278.7	281.2
Predicted (prognostic stage)												
μ_T	286.5	292.0	294.9	299	300.7	296.5	291.2	285.6	280.1	277.6	278.5	281.8
σ_T	1.5	1.5	1.4	1.4	1.4	1.3	1.3	1.3	1.3	1.4	1.4	1.5

Table 2.: Initial priors and process noises of the PF

	C	β	Φ
Initial prior	$\mathcal{N}\left(0, 0^2\right)$	$\mathcal{N}\left(-2640.4, 45^2\right)$	$\mathcal{N}\left(1, 0.7^2\right)$
ε	8.0	500	0.05

Prognostic stage In the prognostic stage the latest state is extrapolated to a failure threshold, using the updated model parameters distributions. Input temperatures need to be approximated, because they are not known for future time steps. Publicly available climate data for Tsukuba, Japan are retrieved from Weather Atlas (2022) to create probability distributions of the monthly average temperature for each month, i.e. $\mathcal{N}\left(\mu_T, \sigma_T^2\right)$. μ_T is the mean monthly average temperature and σ_T is calculated by $\frac{T_{max}-T_{min}}{2}$, with T_{max} and T_{min} the mean maximum and mean minimum monthly temperature respectively. The values for μ_T and σ_T are given in Table 1. For each particle and each future time step a sample is drawn from the distribution of the specific month.

The predicted remaining useful life (RUL) of a single particle can be calculated by subtracting the time step of prediction (t_{pred}) from the time step at which the particle exceeds a failure threshold C_{thr} (t_{thr}):

$$RUL^i = t^i_{thr} - t_{pred} \tag{7}$$

All particles combined, yield a probability distribution of the RUL, including uncertainties of the model (process noises and parameter distributions) and loads (temperature distributions).

4. Results

This section first presents the parameter estimation results obtained by the filter (i.e. during the filtering stage). Then, RUL predictions are given (i.e. the prognostic stage).

Filtering stage The parameter estimates that are obtained during the filtering stage are shown in Fig. 3. The estimates of β are shown in figure 3a and the estimates of Φ are shown in figure 3b. Each figure represents the particle distribution at each time step. Also the average value $\pm$ one standard deviation is visualized. For Φ also its approximated actual value is shown.

To estimate an actual value of Φ, the following procedure is followed. Accelerating factors are calculated for a range of temperatures with k_{nom} and T_{nom} approximated from the ICP database (as selected for Eq. (3a)). Then, accelerating factors are calculated for a range of temperatures with k_{nom} and T_{nom} taken from the NIMS data set (i.e. $k_{nom,actual}$ and $T_{nom,actual}$). Next, it is estimated to which correction factor the accelerating factors retrieved from the ICP initialization needed to be multiplied to match the accelerating factors retrieved from the NIMS initialization. This is the correction factor Φ with an observed value of 0.73.

Up to $t = 5$ months an increase of β is observed in Fig. 3a, which can be interpreted as a decreasing influence of temperature on the corrosion process. As can be seen in Fig. 1 the corrosion process seems to be a fairly linear process up to this point. The PF adapts to the relatively high mass losses with a high value of Φ.

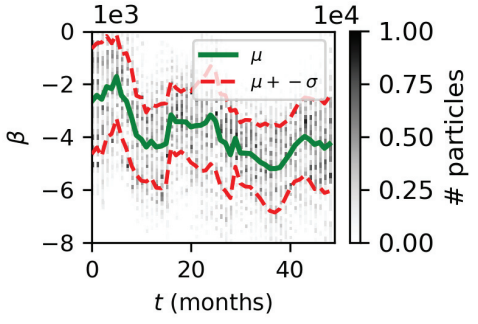

(a) Filtering results β

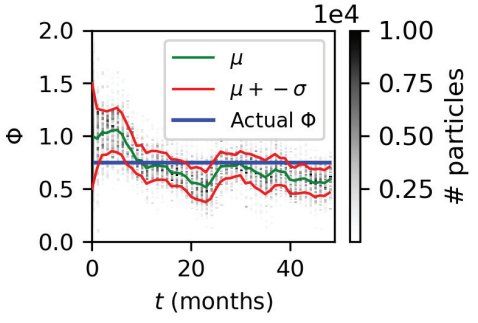

(b) Filtering results Φ

Fig. 3.: Estimated parameters in filtering stage. Grey dots represent groups of particles (gray scale indicates the number of particles).

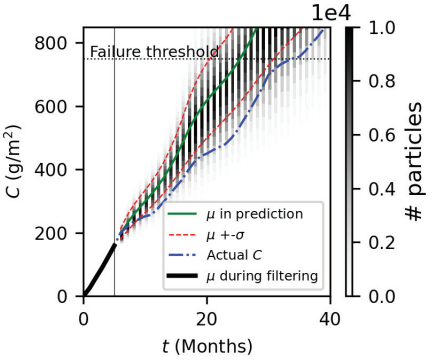

(a) Prediction after 5 months

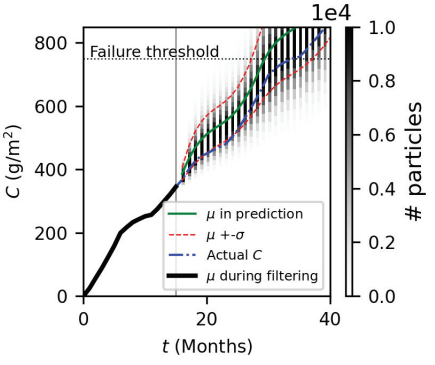

(b) Prediction after 15 months

Fig. 4.: Mass loss predictions at two moments in time by PF. Grey dots represent groups of particles (gray scale indicates number of particles).

In the period after $t = 5$ months, the colder months arrive. Because of the increased variability in temperatures and correlated mass losses, the PF gets mores sensitive to temperature (i.e. β decreases). At this point, the PF also starts to get closer to the actual value of Φ, as Φ does not need to compensate for temperature effects anymore.

After β has reached the valley around $t = 10$ months the parameters keep fluctuating and do not converge to one value. This is due to the fact that the corrosion process is highly uncertain and noisy. Parameter convergence in Bayesian filters is only obtained when the degradation model and its governing loads are fully defined (Keizers et al., 2021). Because of the uncertain corrosion model which does not include all governing loads, the degradation model is not fully defined and adaptivity remains. Still, the PF improved the degradation model with respect to the initially proposed prior. This is shown by the fact that the estimation of Φ shifts towards the approximated actual value of Φ and the temperature-related variation is captured better.

Prognostic stage The parameter distributions obtained in the filtering stage are used in the prognostic stage to propagate particles up to a mass loss threshold C_{thr}, which is arbitrary set to 750g/cm^2. Results of prognostics from two different time steps are given in Fig. 4. The particle distributions and the mean $\pm$ one standard deviation are plotted again at each time step. Fig. 4a shows

the prediction after $t = 5$ months, where the PF had only observed few variations in temperatures end mass losses and a high value of β and Φ was observed (see Fig. 3). Due to the high value of β the temperature fluctuations only have limited effect on the corrosion predictions, which is represented by a relatively linear trend. The high value of Φ makes that the PF overestimates the actual mass loss.

Fig. 4b shows the prediction after $t = 15$ months. At this point the prediction shows non-linear (wavy) behavior, which reveals that the changing temperatures significantly affect the corrosion process. The increased effect due to temperature changes is expected, given the lower value of β observed in Fig. 3a.

The prediction results show that the PF can predict the corrosion process reasonably well, while only requiring a simple model with only one input parameter (T). This is emphasized by Fig. 5, which shows the predicted RUL at each time step, as well as the actual RUL at that time step. It is observed that the actual RUL is always within one standard deviation from the mean, except for the initial period in which the PF did not observe colder months yet. First, the predicted RUL approaches the actual RUL. After $t = 17$ months the PF diverges from the actual RUL, because at this point the PF adapts to colder months leading to an overestimation of the RUL. During the last months convergence to the actual RUL is observed.

5. Discussion

The capabilities of the PF for corrosion prognostics are demonstrated. Now two major considerations for practical implementation are discussed.

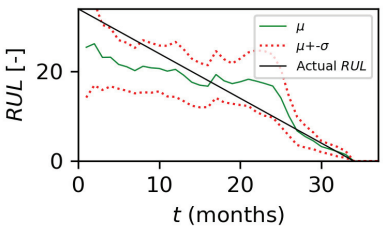

Fig. 5.: RUL predicted by PF at each time step.

Setting-up a particle filter in new applications In this work the model parameters, the number of particles, the priors and the process noises could be tuned to obtain a robust and accurate filter because the corrosion data was known in advance. However, in new practical applications this is not the case and a filter needs to be developed from scratch. Parameter selection needs to be done based on expert knowledge or physics, which is no trivial task due to the complex physics of corrosion. Good understanding of the effect of environmental factors in specific environments is required. Also uncertainties in the process need to be selected based on expert knowledge or physical understanding. This emphasizes the importance of further research on the fundamentals of corrosion and development of corrosion data sets in various environments.

Long-term corrosion This work considered a continuous corrosion process, but long-term corrosion effects were neglected. Formation of a protective (rust) layer has a significant influence on the corrosion process and should therefore not be neglected when the method is applied in practice. Unfortunately there is a lack of transient corrosion data sets in which long-term corrosion is measured frequently. Development of new corrosion monitoring devices can help to generate long-term corrosion data sets which can be used to apply and verify PFs. Because the ability of a PF to learn in real-time, it is expected that it can be used to learn both environmental influences and long-term corrosion effects simultaneously.

6. Conclusion and Future Work

A PF was proposed for atmospheric corrosion prognostics, for which it has been demonstrated: (i) with only few input parameters, a probability distribution of the RUL can be obtained; (ii) the method takes into account uncertainties in the process, the model parameters and future weather conditions and shows therefore good applicability for a complex and uncertain process like corrosion; (iii) since the physics of the process could not be described exactly by a model, the PF remained adaptive to its environment, yielding

slight (but acceptable) deviations of the RUL in specific situations; (iv) application of the filter to new practical cases is not trivial, and requires parameter selection based one expert knowledge or physics; (v) long-term corrosion effects have been neglected, but can be included in the method once relevant data sets become available.

Future research will have to focus on more fundamental underpinning of the model parameter selection process. Furthermore, an actual long-term corrosion data set would be required to validate the methodology. Finally, this paper showed the possibility to predict corrosion using a PF, but did not yet compare the strategy to other approaches. This comparison will be made in future work.

Acknowledgements

The authors thank the National Institute for Materials Science gratefully for making the Data Sheet on Atmospheric Corrosion Properties of Carbon Steels Obtained from Short Term Exposure Test (NIMS, 2011) publicly available within the MatNavi Corrosion Data Sheets.

This work is part of the PrimaVera Project, which is partly financed by the Dutch Research Council (NWO) under grant agreement NWA.1160.18.238.

References

Arrhenius, S. (1889). Über die dissociationswärme und den einfluss der temperatur auf den dissociationsgrad der elektrolyte. *4*(1), 96–116.

Arulampalam, M., S. Maskell, N. G. , and T. Clapp (2002). A tutorial on particle filters for online nonlinear/non-gaussian bayesian tracking. *IEEE Transactions on Signal Processing 50*(2), 174–188.

Cai, Y., Y. Xu, Y. Zhao, and X. Ma (2020). Atmospheric corrosion prediction: a review. *CORROSION REVIEWS 38*(4), 299–321.

Cai, Y., Y. Xu, Y. Zhao, and X. Ma (2021, July). Extrapolating short-term corrosion test results to field exposures in different environments. *Corrosion Science 186*, 1–14.

Chen, Z. (2003). Bayesian filtering: From kalman filters to particle filters, and beyond. *Statistics 182*(1), 1–69.

Chico, B., D. De la Fuente, I. Díaz, J. Simancas, and M. Morcillo (2017). Annual atmospheric corrosion of carbon steel worldwide. an integration of isocorrag, icp/unece and micat databases. *Materials 10*(6), 1–26.

Elfring, J., E. Torta, and R. van de Molengraft (2021). Particle filters: A hands-on tutorial. *Sensors 21*(2), 1–28.

ICP (1987). Materials reports. `https://www.ri.se/en/icp-materials/documents/icp-materials-reports`. Retrieved on 02-03-2022.

Keizers, L. S., R. Loendersloot, and T. Tinga (2021). Unscented kalman filtering for prognostics under varying operational and environmental conditions. *International Journal of Prognostics and Health Management 12*(2), 1–20.

Melchers, R. E. (2019). Predicting long-term corrosion of metal alloys in physical infrastructure. *npj Materials Degradation 3*(4), 1–7.

NIMS (2011). Data sheet on atmospheric corrosion properties of carbon steels obtained by short term exposure tests. `https://mits.nims.go.jp/en/`. Retrieved on 17-02-2021.

Pei, Z., X. Cheng, X. Yang, Q. Li, C. Xia, D. Zhang, and X. Li (2021, Feb). Understanding environmental impacts on initial atmospheric corrosion based on corrosion monitoring sensors. *Journal of Materials Science & Technology 64*, 214–221.

Tinga, T. (2013). *Principles of Loads and Failure Mechanisms. Applications in Maintenance, Reliability and Design*. Springer.

Weather Atlas (2022). Monthly weather forecast and climate tsukuba, japan. `https://www.weather-atlas.com/en/japan/tsukuba-climate`. Retrieved on 05-01-2022.